AIAA JOURNAL
Vol. 34, No. 9, September 1996

Nonlinear Response of Long Orthotropic Tubes Under Bending Including the Brazier Effect

Brian F. Tatting* and Zafer Gürdal†
Virginia Polytechnic Institute and State University, Blacksburg, Virginia 24061-0219
and
Valery V. Vasiliev‡
Moscow State University of Aviation Technology, Moscow, Russia

A nonlinear solution to the Brazier problem of cross-sectional flattening for infinitely long tubes under bending is formulated using classical nonlinear shell theory along with semimembrane constitutive relations. It is shown that traditional cylindrical shell equations are not sufficient to accurately model the nonlinearity of the Brazier effect, and the suitable corrections to the shell equations are derived. This approach gives greater physical insight into the problem than traditional variational methods, and it yields a highly nonlinear ordinary differential equation for infinite length cylinders with orthotropic material properties. This resulting equation is solved numerically using finite difference techniques, and an approximate analytical solution is also obtained, which corresponds to Brazier's original solution. Collapse loads as a result of limit points and local instability are compared with classical failure estimates, and the influences of laminate stacking sequence and internal pressure are explored. Also, a collapse parameter is introduced that gives a relative measure of the buckling load to that of the limit load for orthotropic structures, and it is shown that, for low values of this parameter, the limit moment is not a suitable estimate for the collapse load of long cylinders.

Introduction

THE Brazier effect can be easily demonstrated by simply bending a drinking straw or rubber hose by hand. As the curvature of the tube increases, one can feel that the applied moment needed to produce this extra curvature begins to lessen, and often a change in the shape of the cross section of the tube may be observed. Finally, the tube will form a kink and collapse. This phenomenon was first investigated by Brazier,[1,2] and he formulated a solution to explain the flattening behavior of isotropic circular cylinders under bending. This cross-sectional deformation is a result of the line of action of the longitudinal stresses in a long tube in conjunction with the curvature of the tube axis. For example, an infinitesimal section of a deformed tube along with the linear stress state associated with pure bending is shown in Fig. 1. The compressive stresses at the top generate a downward force on the cross section because of the curvature of the tube axis, whereas the tensile stresses at the bottom produce a similar upward force. These forces combine to flatten the original circular cross section into an oval, thus decreasing the moment of inertia of the cross section and producing a nonlinear load–displacement relation. Eventually, the applied moment exceeds the load-carrying capability of the ovalized cross section, and the tube collapses. In practice, however, this limit moment is often never reached, because the flattening of the cross section also lowers the structure's local buckling load, which generates a kink that leads to failure. The load required to produce a limit moment and/or generate the formation of this kink must be accurately determined for reliable design of long orthotropic cylinders under bending.

The infinite cylindrical shell is the problem originally studied by Brazier. It could also be construed as a greased end cylinder in which radial and circumferential displacements are allowed at each end. Applications for this idealized problem include underwater pipes, medical tubing, and long cylinders subjected to beam loading, such as fuselage structures or submarine hulls.

Received July 28, 1995; revision received March 19, 1996; accepted for publication March 22, 1996.

*Ph.D. Candidate, Department of Engineering Science and Mechanics. Student Member AIAA.
†Professor, Department of Engineering Science and Mechanics. Associate Fellow AIAA.
‡Head, Department of Aerospace Composite Structures.

The shell analysis used here is based on Vlasov's semimembrane theory (e.g., see Ref. 3). This simplified constitutive theory neglects bending of the shell wall in the axial direction, thereby eliminating the boundary layer present in usual shell problems. Semimembrane theory also neglects the Poisson effect and assumes the circumferential and shear strain to be zero. Its application is for long shells or shells in which the variation of stresses and strains is slow in the axial direction. These conditions are certainly satisfied for the infinite tube case. Other notable investigators who have utilized the semimembrane theory for the solution of the Brazier problem include Aksel'rad and Emmerling[4] and Libai and Bert.[5]

An additional mode of structural failure that is not considered here is a result of violation of material strength criteria of the laminate (see, for instance, Ref. 6). Consideration of this failure aspect would require stipulation of specific material systems and cylinder geometries, which is not within the scope of this paper. However, the analysis presented can be easily modified to include estimations of material failure because of any criterion, which will be required in the optimization process.

The goal of this paper is to develop the governing equations for an infinite length orthotropic cylinder under pure bending from classical nonlinear shell equations. This derivation should give greater physical insight into the mechanics of the Brazier effect than usual variational methods, as well as provide a consistent approach to explore more complicated tube bending problems, such as arbitrary cross sections, general beam loading conditions, and the influence of stiffeners and end conditions in the axial direction. Additionally, the influence of laminate stacking sequence and internal pressure on the collapse loads of orthotropic structures needs to be explored to discover optimal configurations for typical stiffened cylindrical structures under flexural loading.

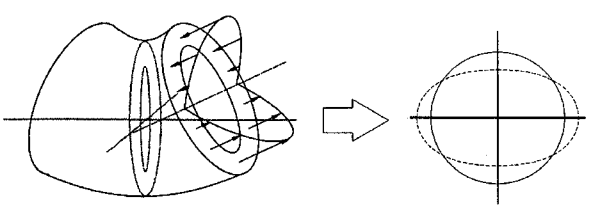

Fig. 1 Mechanism of Brazier effect to produce ovalization.

Nonlinear Analysis for Infinite Shell

We begin with the derivation of the particular nonlinear strain–displacement relations for an infinitely long circular cylinder under bending. Attention is focused on the cross-sectional deformation of a tube with a constant axial curvature and dimensions of mean radius R and shell thickness H (see Fig. 2). Here (u_x, u_y, u_z) denote displacements in the Cartesian (rectangular) coordinate directions, whereas the symbols (u, v, w) represent cylindrical coordinate displacements. The function $f_1(x)$ shown in Fig. 2 represents the axial profile of some reference line (*ref*) in the shell, which is made to correspond to the neutral surface of the cross section and is usually taken as $\theta_{\text{ref}} = \pi/2$. Under pure bending, the curvature of this axial profile ($\kappa \equiv d^2 f_1/dx^2$) is constant along the length of this infinite tube. Also note that the compressive stress state is located at the top of the structure, which corresponds to $\theta = 0$.

The general strain–displacement relations for a circular cylinder expressed in rectangular coordinates is given as

$$\varepsilon_x = \frac{\partial u_x}{\partial x} + \frac{1}{2}\left(\frac{\partial u_x}{\partial x}\right)^2 + \frac{1}{2}\left(\frac{\partial u_y}{\partial x}\right)^2 + \frac{1}{2}\left(\frac{\partial u_z}{\partial x}\right)^2$$

$$\varepsilon_\theta = \cos\theta\left(\frac{1}{R}\frac{\partial u_y}{\partial \theta}\right) - \sin\theta\left(\frac{1}{R}\frac{\partial u_z}{\partial \theta}\right) + \frac{1}{2}\left(\frac{1}{R}\frac{\partial u_x}{\partial \theta}\right)^2 + \frac{1}{2}\left(\frac{1}{R}\frac{\partial u_y}{\partial \theta}\right)^2 + \frac{1}{2}\left(\frac{1}{R}\frac{\partial u_z}{\partial \theta}\right)^2 \tag{1}$$

$$\gamma_{x\theta} = \frac{1}{R}\frac{\partial u_x}{\partial \theta} + \cos\theta\frac{\partial u_y}{\partial x} - \sin\theta\frac{\partial u_z}{\partial x} + \left(\frac{1}{R}\frac{\partial u_x}{\partial \theta}\right)\left(\frac{\partial u_x}{\partial x}\right) + \left(\frac{1}{R}\frac{\partial u_y}{\partial \theta}\right)\left(\frac{\partial u_y}{\partial x}\right) + \left(\frac{1}{R}\frac{\partial u_z}{\partial \theta}\right)\left(\frac{\partial u_z}{\partial x}\right)$$

Now we will assume that the only nonlinear terms that are important are those dealing with cross-sectional deformation. That is,

$$\frac{\partial u_x}{\partial x} \ll 1 \qquad \frac{\partial u_y}{\partial x} \ll 1 \qquad \frac{\partial u_z}{\partial x} \ll 1 \qquad \frac{\partial u_x}{\partial \theta} \ll 1 \tag{2}$$

Therefore, the nonlinear strains are represented as

$$\varepsilon_x = \frac{\partial u_x}{\partial x}$$

$$\varepsilon_\theta = \cos\theta\left(\frac{1}{R}\frac{\partial u_y}{\partial \theta}\right) - \sin\theta\left(\frac{1}{R}\frac{\partial u_z}{\partial \theta}\right) + \frac{1}{2}\left(\frac{1}{R}\frac{\partial u_y}{\partial \theta}\right)^2 + \frac{1}{2}\left(\frac{1}{R}\frac{\partial u_z}{\partial \theta}\right)^2 \tag{3}$$

$$\gamma_{x\theta} = \frac{1}{R}\frac{\partial u_x}{\partial \theta} + \cos\theta\frac{\partial u_y}{\partial x} - \sin\theta\frac{\partial u_z}{\partial x} + \frac{1}{R}\left(\frac{\partial u_y}{\partial \theta}\right)\left(\frac{\partial u_y}{\partial x}\right) + \frac{1}{R}\left(\frac{\partial u_z}{\partial \theta}\right)\left(\frac{\partial u_z}{\partial x}\right)$$

These strains can also be expressed in terms of the cylindrical coordinate displacements (u, v, w), which are defined from the Cartesian displacements as

$$u = u_x \qquad v = u_y\cos\theta - u_z\sin\theta \qquad w = u_y\sin\theta + u_z\cos\theta \tag{4}$$

Thus from Eqs. (3) and (4) the strains are also written as

$$\varepsilon_x = \frac{\partial u}{\partial x}$$

$$\varepsilon_\theta = \left(\frac{1}{R}\frac{\partial v}{\partial \theta} + \frac{w}{R}\right) + \frac{1}{2}\left(\frac{1}{R}\frac{\partial v}{\partial \theta} + \frac{w}{R}\right)^2 + \frac{1}{2}\left(\frac{v}{R} - \frac{1}{R}\frac{\partial w}{\partial \theta}\right)^2 \tag{5}$$

$$\gamma_{x\theta} = \frac{1}{R}\frac{\partial u}{\partial \theta} + \frac{\partial v}{\partial x} + \left(\frac{1}{R}\frac{\partial v}{\partial \theta} + \frac{w}{R}\right)\left(\frac{\partial v}{\partial x}\right) - \left(\frac{v}{R} - \frac{1}{R}\frac{\partial w}{\partial \theta}\right)\left(\frac{\partial w}{\partial x}\right)$$

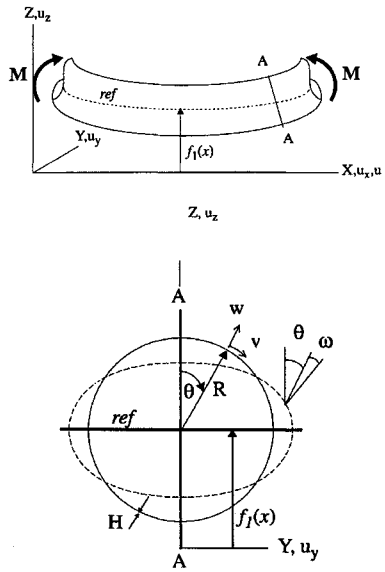

Fig. 2 Geometry of deformed shell.

Next we must consider the change in curvature in the circumferential direction of a shell element, which will be in terms of the circumferential rotation ω (for definition of positive rotation see Fig. 2). We will utilize Brazier's assumption that the deformation of the cross section contour is inextensional; i.e., there is no stretching in the circumferential direction. First, note that the undeformed circular cross section can be defined by

$$\frac{1}{R} = \frac{d\theta}{ds} \tag{6}$$

where ds is the arclength. Since this arclength remains the same in both cases because of the inextensionality condition, the definition of the deformed cross section can be expressed as

$$\frac{1}{R_\theta} = \frac{d(\omega + \theta)}{ds} \tag{7}$$

Therefore the change in curvature is simply

$$\kappa_\theta = \frac{1}{R_\theta} - \frac{1}{R} = \frac{d\omega}{ds} = \frac{1}{R}\frac{d\omega}{d\theta} \tag{8}$$

Furthermore, we can relate the inextensional rotation ω to the displacements of a point in the cross section, since (from Fig. 2)

$$R\sin(\omega + \theta) = -\frac{\partial Z}{\partial \theta} = R\sin\theta - \frac{\partial u_z}{\partial \theta}$$
$$R\cos(\omega + \theta) = \frac{\partial Y}{\partial \theta} = R\cos\theta - \frac{\partial u_y}{\partial \theta} \tag{9}$$

Enforcing the symmetry condition and the definition of the neutral (reference) surface

$$u_y|_{\theta=0} = 0 \qquad u_z|_{\theta=\theta_{\text{ref}}} = f_1(x) \tag{10}$$

results in integral equations for the Cartesian displacements

$$u_y = R\eta(\theta) \qquad u_z = f_1(x) - R\phi(\theta)$$
$$\eta(\theta) = \int_0^\theta [\cos(\omega + \theta) - \cos\theta]\, d\theta \tag{11}$$
$$\phi(\theta) = \int_{\theta_{\text{ref}}}^\theta [\sin(\omega + \theta) - \sin\theta]\, d\theta$$

where we have defined η and ϕ as the nondimensional horizontal and vertical cross-sectional displacements, respectively. The cylindrical-

coordinate cross-sectional displacements (v, w) can also be formulated in terms of the nonlinear rotation ω, through Eq. (4):

$$v(x,\theta) = R(\eta\cos\theta + \phi\sin\theta) - f_1(x)\sin\theta$$
$$w(x,\theta) = R(\eta\sin\theta - \phi\cos\theta) + f_1(x)\cos\theta \tag{12}$$

Additionally, the nonlinear expression for the circumferential strain in Eq. (5) is composed of two portions, namely the linear strain and rotation. Using Eq. (12), we express these portions of the circumferential strain as

$$\frac{1}{R}\left(\frac{\partial v}{\partial\theta} + w\right) = \cos\omega - 1$$
$$\frac{1}{R}\left(v - \frac{\partial w}{\partial\theta}\right) = \sin\omega \tag{13}$$

Note that the nonlinear circumferential strain of Eq. (5) is identically zero as expected.

To express the axial displacement in terms of ω, we must utilize one more assumption: the shear strain $\gamma_{x\theta}$ is zero. This will be true for infinite cylinders under pure bending, since there are no end conditions or shear forces on the structure to produce shear stresses. Then we can set $\gamma_{x\theta}$ to zero in Eq. (3), employ Eq. (11), and integrate for the axial displacement u, which is used to define the axial strain:

$$u = -R\frac{\mathrm{d}f_1}{\mathrm{d}x}(\cos\theta - \phi) + f_2(x)$$
$$\varepsilon_x = -R\frac{\mathrm{d}^2 f_1}{\mathrm{d}x^2}(\cos\theta - \phi) + \frac{\mathrm{d}f_2}{\mathrm{d}x} \tag{14}$$

$f_2(x)$ is a constant of integration over θ and corresponds to axial displacement at the reference line. Thus all of the displacements and in-plane strain quantities can be expressed in terms of the reference surface displacements $f_1(x)$ and $f_2(x)$ and the nonlinear rotation $\omega(\theta)$.

The stress–strain behavior for these shells is based on classical lamination theory along with the semimembrane assumptions mentioned earlier. Macroscopic laminate stiffness measures are determined by integrating through the thickness of the shell wall in the usual manner. In particular, we calculate the extensional and bending stiffnesses as

$$A_{ij} = \int_{-H/2}^{H/2} \bar{Q}_{ij}\,\mathrm{d}z \qquad D_{ij} = \int_{-H/2}^{H/2} \bar{Q}_{ij} z^2\,\mathrm{d}z \tag{15}$$

where $\bar{Q}_{ij}$ are the transformed reduced stiffnesses of an orthotropic layer (see, e.g., Ref. 7). We restrict our investigation to balanced symmetric laminates.

We now invoke the assumptions of semimembrane constitutive theory. First, shell bending and twisting in the axial direction are ignored, and the Poisson effect is neglected. This can be expressed mathematically as

$$D_{11}, D_{12}, D_{16}, D_{26}, D_{66} \to 0 \tag{16}$$

Thus, the bending and twisting moments in the axial direction (M_x, M_{xy}) are zero. Since the Poisson effect is neglected, the in-plane stress resultants depend only on their corresponding strain measures:

$$N_x = E_x H\varepsilon_x \qquad N_\theta = E_\theta H\varepsilon_\theta \qquad N_{x\theta} = A_{66}\gamma_{x\theta} \tag{17}$$

We have defined the effective moduli for orthotropic laminates in terms of the extensional stiffness measures to include arbitrary laminate layups:

$$E_x = \frac{A_{11}A_{22} - A_{12}^2}{A_{22}H} \qquad E_\theta = \frac{A_{11}A_{22} - A_{12}^2}{A_{11}H} \tag{18}$$

Finally, the assumptions of inextensionality of the cross section and lack of shear strain can be stipulated at the constitutive level as

$$E_\theta, A_{66} \to \infty \Rightarrow \varepsilon_\theta, \gamma_{x\theta} = 0 \tag{19}$$

From these remarks, it is evident that the only necessary constitutive relations are

$$N_x = E_x H\varepsilon_x \qquad M_\theta = D_{22}\kappa_\theta \tag{20}$$

With the definition of the axial stress resultant N_x, the total axial force and applied bending moment over the cross section of the structure can be found from

$$N = \oint N_x R\,\mathrm{d}\theta = 0$$
$$M = -\oint N_x(R\cos\theta + u_z)R\,\mathrm{d}\theta \tag{21}$$

The first equation calculates the axial strain at the reference surface [see Eq. (14)], whereas the second supplies the nonlinear relation between the curvature of the tube axis ($\kappa = \mathrm{d}^2 f_1/\mathrm{d}x^2$) and applied bending moment:

$$\frac{\mathrm{d}f_2}{\mathrm{d}x} = (R\kappa)\left[\frac{1}{2\pi}\oint(\cos\theta - \phi)\,\mathrm{d}\theta\right]$$
$$R\kappa\oint(\cos\theta - \phi - \cos\theta_{\mathrm{ref}})^2\,\mathrm{d}\theta = \frac{M}{E_x HR^2} \tag{22}$$

These are the beam equations for a circular cylinder with the Brazier effect included. The function $f_2(x)$ and constant κ exactly correspond to axial extension and curvature of a one-dimensional beam. If we ignore the Brazier phenomenon, the preceding equations reduce to elementary beam theory, as expected:

$$\frac{\mathrm{d}f_2}{\mathrm{d}x} = 0 \qquad \kappa = \frac{M}{EI} \tag{23}$$

Furthermore, we desire θ_{ref} to correspond to the neutral surface under bending, such that $\varepsilon_x(\theta = \theta_{\mathrm{ref}}) = 0$. Thus we utilize the first of Eq. (22) along with Eq. (14) to define the location of the reference surface:

$$\cos\theta_{\mathrm{ref}} = \frac{1}{2\pi}\oint(\cos\theta - \phi)\,\mathrm{d}\theta \tag{24}$$

Lastly, we will need the nonlinear equilibrium equations to generate the governing equation for ω. Again there are simplifications of the equations as a result of the restrictions of semimembrane theory, which only includes the bending moment and shear force that are in the circumferential direction. Moreover, we will not include terms containing derivatives in the axial direction, since we are assuming an infinite shell that does not have stress or strain variation along the length. Then the shell equilibrium equations become (see Ref. 3)

$$\frac{\partial}{\partial\theta}(A_1 N_\theta) - \frac{\partial A_1}{\partial\theta}N_x + \frac{A_1 A_2}{R_\theta}Q_\theta = 0$$
$$\frac{\partial}{\partial\theta}(A_1 N_{x\theta}) + \frac{\partial A_1}{\partial\theta}N_{x\theta} = 0$$
$$\frac{\partial}{\partial\theta}(A_1 M_\theta) - A_1 A_2 Q_\theta = 0$$
$$\frac{\partial}{\partial\theta}(A_1 Q_\theta) - A_1 A_2\left(\frac{N_\theta}{R_\theta} + \frac{N_x}{R_x}\right) + A_1 A_2 p = 0 \tag{25}$$

Here (A_1, A_2) and (R_x, R_θ) are the Lamé coefficients and Gaussian radii of curvature of the surface defined by the shell in (x, θ) coordinates. In the standard nonlinear formulation for cylindrical shells, these surface parameters are calculated as

$$A_1 = 1 \qquad \frac{1}{R_x} = \kappa_x = \frac{\mathrm{d}^2 f_1}{\mathrm{d}x^2}\cos\theta$$
$$A_2 = R \qquad \frac{1}{R_\theta} = \frac{1}{R} + \kappa_\theta = \frac{1}{R}\left(1 + \frac{\partial\omega}{\partial\theta}\right) \tag{26}$$

However, the driving mechanism for the Brazier effect relies on the action of the axial stresses along with the curvature of the axis and shape of the cross section. Thus the surface parameters must be derived by assuming a cylindrical shell with some axial curvature

and cross-sectional deformation. Referring to the geometry of Fig. 2, we assume that the cross section rotates through an angle equal to the slope of the reference line, df_1/dx. Then the expressions for the shape of the deformed shell become

$$X = x - R\sin\left(\frac{df_1}{dx}\right)(\cos\theta - \phi - \cos\theta_{\text{ref}})$$
$$Y = R(\sin\theta + \eta) \tag{27}$$
$$Z = f_1(x) + R\cos\left(\frac{df_1}{dx}\right)(\cos\theta - \phi - \cos\theta_{\text{ref}})$$

Calculation of the Lamé coefficients and Gaussian curvatures in the usual manner (e.g., see Ref. 8), along with the assumption of small cross-sectional rotations, gives the following expressions for A_1 and R_x:

$$A_1 = 1 - \kappa R(\cos\theta - \phi - \cos\theta_{\text{ref}})$$
$$\frac{1}{R_x} = \frac{-\kappa\cos(\omega+\theta)}{1 - \kappa R(\cos\theta - \phi - \cos\theta_{\text{ref}})} \tag{28}$$

Note that these differ from the usual Lamé parameters for circular cylindrical shells since $\partial A_1/\partial\theta \neq 0$ here.

The four equilibrium equations, Eq. (25), can now be combined into one nonlinear equation involving only M_θ and N_x through integration and application of symmetry conditions. Some terms can also be neglected because of their relative size. For instance, the equilibrium equations contain many terms that are multiplied by A_1. However, since κR is much smaller than unity, we can neglect the second part of A_1 for most terms. The exception is when A_1 has circumferential derivatives that are multiplied by N_x. This derivative of A_1 is not equal to zero [though it is for traditional nonlinear cylindrical shell equations as in Eq. (26)], and the multiplication of it with the largest stress measure generates a term that cannot be neglected. In fact, omission of this term will lead to a solution off by a factor of $\frac{2}{3}$. Thus traditional cylindrical shell equilibrium equations are not sufficient to model the nonlinearity of the Brazier effect but must be modified to include this important nonlinear term.

Following this argument, the second equilibrium equation (along with a symmetry condition) becomes

$$\frac{\partial}{\partial\theta}(N_{x\theta}) = 0 \qquad N_{x\theta}|_{\theta=0} = 0 \tag{29}$$

Solution of this differential equation and application of the homogeneous symmetry condition determine that $N_{x\theta} = 0$ at all locations. Thus the semimembrane assumption of zero shear strain (and zero shear stress) is valid for infinite length cylinders. It should be reemphasized, however, that this assumption is not valid for finite length cylinders or for arbitrary beam loading.

Referring back to Eq. (25), we can express the intermediate variables N_θ and Q_θ through the third and fourth equilibrium equations as

$$Q_\theta = \frac{1}{R}\frac{\partial M_\theta}{\partial\theta}$$
$$N_\theta = R_\theta\frac{1}{R}\frac{\partial Q_\theta}{\partial\theta} + pR_\theta - \frac{R_\theta}{R_x}N_x \tag{30}$$

where N_θ and Q_θ are nonzero stress measures that are defined through the equilibrium equations, yet do not follow a constitutive law because of the assumptions of semimembrane theory. Insertion of these stress measures into the first equilibrium equation yields a governing equation for N_x and M_θ:

$$\frac{1}{R}\frac{\partial}{\partial\theta}\left[\frac{R_\theta}{R^2}\frac{\partial^2 M_\theta}{\partial\theta^2}\right] + \frac{1}{R_\theta R}\frac{\partial M_\theta}{\partial\theta} + \frac{1}{R}\frac{\partial}{\partial\theta}(pR_\theta)$$
$$= \frac{1}{R}\frac{\partial A_1}{\partial\theta}N_x + \frac{1}{R}\frac{\partial}{\partial\theta}\left[\frac{A_1 R_\theta}{R_x}N_x\right] \tag{31}$$

Substitution of the constitutive laws for N_x and M_θ along with the definitions of ε_x and κ_θ yield a fourth-order ordinary differential equation (ODE) for ω. Let us now define some nondimensional parameters:

$$\bar{\alpha} = \frac{\kappa R^2 E_x H}{2\sqrt{D_{11}E_\theta H}} \qquad \bar{m} = \frac{M}{2\pi R\sqrt{D_{11}E_\theta H}}$$
$$\bar{p} = \frac{pR^3}{3D_{22}} \qquad n_x = \frac{-N_x R}{2\sqrt{D_{11}E_\theta H}} \tag{32}$$

where the curvature, bending moment, pressure, and axial stress resultant have all been normalized with respect to their classical buckling values for an infinite cylinder. We will also introduce a parameter χ that is a function of laminate stacking sequence:

$$\chi = \sqrt{\frac{D_{11}E_\theta}{D_{22}E_x}} \tag{33}$$

Then the differential equation for ω becomes (a prime represents $d/d\theta$)

$$\left(\frac{\omega'''}{1+\omega'}\right)' + (1+\omega')\omega'' + \left(\frac{3\bar{p}}{1+\omega'}\right)'$$
$$= 4\chi^2\bar{\alpha}\left\{\left[\frac{n_x\cos(\omega+\theta)}{1+\omega'}\right]' - n_x\sin(\omega+\theta)\right\} \tag{34}$$

with the auxiliary relations

$$n_x(\theta) = \bar{\alpha}(\cos\theta - \phi - \cos\theta_{\text{ref}})$$
$$\bar{m} = \frac{\bar{\alpha}}{\pi}\left[\oint(\cos\theta - \phi - \cos\theta_{\text{ref}})^2\,d\theta\right] \tag{35}$$

This is precisely the equation found by Reissner[9] (for isotropic materials), except that he introduced the nonlinear loading terms (containing $\bar{\alpha}^2$) through a less rigorous approach. He then solved the nonlinear equation approximately using perturbation techniques. A numerical solution of this equation was performed by Fabian.[10] Linearization of this equation in terms of a Fourier expansion for the radial displacement w leads to the original ODE discovered by Brazier. His simplistic solution establishes that the radial displacement varies as $\cos(2\theta)$ and is of the form (Wood[11] later included the effects of pressure)

$$\bar{m} = \bar{\alpha}\left[1 - \frac{\chi^2\bar{\alpha}^2}{2(1+\bar{p})}\right]$$
$$\bar{w}(\theta) = -\frac{w(\theta)}{R} = \frac{\chi^2\bar{\alpha}^2}{3(1+\bar{p})}\cos 2\theta \tag{36}$$

Solution for the full nonlinear shell equation is shown in Fig. 3 for an isotropic material under pure bending ($\chi = 1$ and $\bar{p} = 0$).

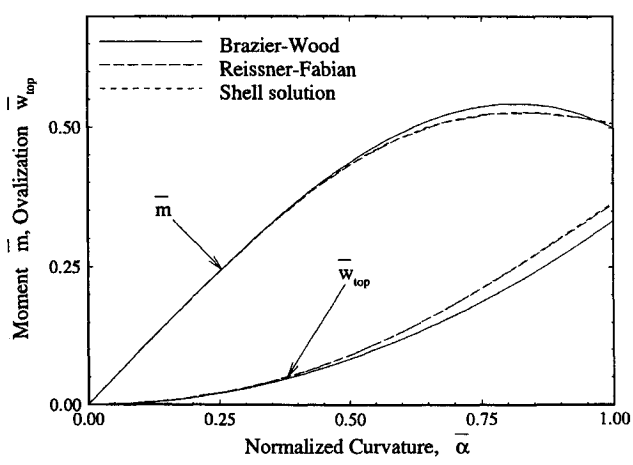

Fig. 3 Moment and ovalization vs curvature for long isotropic cylinder.

[The ovalization of the cross section is usually measured by the radial displacement at $\theta = 0$, which corresponds to $\bar{w}_{\text{top}} = \phi(0)$ for the shell solution.] The solution was obtained using finite difference techniques along with Newton's method. As expected, the results agree exactly with the numerical solution of Fabian, who used similar techniques but also introduced the loading through ad hoc methods. One can also see that the linearized Brazier solution gives excellent results despite its simplicity and provides a tremendous gain in computational efficiency. Similar agreement is observed between the shell solution and Brazier's approximation for all values of χ and $\bar{p}$. A thorough discussion of why this rough solution of Brazier generates such well-behaved results can be found in Calladine.[12]

Limit Points and Local Instability

Often it is believed that the highest point on the nonlinear load path corresponds to the collapse moment for long tubes under bending. Once the maximum bending moment is surpassed, the structure has no ability to withstand the load, and catastrophic failure occurs. Calculation of this limit point is easily accomplished using Brazier's approximation, Eq. (36). The moment reaches a maximum when $d\bar{m}/d\bar{\alpha} = 0$; thus,

$$\bar{\alpha}_{\text{lim}} = \frac{1}{\chi}\sqrt{\frac{2(1+\bar{p})}{3}} \qquad \bar{m}_{\text{lim}} = \frac{2}{3\chi}\sqrt{\frac{2(1+\bar{p})}{3}} \tag{37}$$

Though this limit load is theoretically true for some structures, ones in which the Brazier effect is very pronounced (e.g., large values of χ), most tubes collapse before the limit moment is reached because of the formation of a kink, which represents a postbuckled state. The mechanism that produces this kink is local buckling on the compressive side of the tube. However, the Brazier effect still plays a significant role in this failure mode, for the development of the kink depends substantially on the local curvature of the cross section. It was precisely this behavior that motivated Aksel'rad[13] to determine cylinder collapse loads with this nonlinear deformation.

Buckling of circular cylinders under bending was most qualitatively defined by Seide and Weingarten.[14] They determined that the maximum critical bending stress is roughly equal to the critical buckling stress under axial compression. Local buckling occurs when the maximum compressive stress (at $\theta = 0$) attains this value. For orthotropic materials, this critical stress is

$$\sigma_{\text{cr}} = \frac{-2\sqrt{D_{11}E_\theta H}}{\rho H} \tag{38}$$

where ρ is the local radius of curvature at $\theta = 0$. However, because of the Brazier effect, the cross section of the cylinder deforms into an oval (see Fig. 1), and the radius of curvature at the critical location increases, thus lowering the critical buckling stress. Therefore, one can get a good estimate of the collapse moment by determining when the axial stress on the compressive side of the cylinder reaches this critical value. Of course, a more reliable determination of the collapse load would be to perform a stability analysis from the nonlinear prebuckled state. However, we will employ this Seide–Weingarten approximation[14] since it is computationally simple and reveals the important points of local buckling in a straightforward manner. To make the equations simpler, we will also utilize the linearized equations instead of the highly complex nonlinear solution.

Only two characteristics of the loaded cylinder need be known to determine this approximate stability criterion: circumferential curvature and the axial stress resultant. Both quantities have been defined earlier [see Eqs. (8) and (35)] in terms of the circumferential rotation $\omega(\theta)$. For the linearized Brazier solution, this quantity is calculated to be

$$\omega(\theta) = -\frac{\chi^2\bar{\alpha}^2}{2(1+\bar{p})}\sin 2\theta \tag{39}$$

Therefore the circumferential curvature and axial stress resultant become

$$\begin{aligned} \bar{\kappa}_\theta &= R\kappa_\theta = -\frac{\chi^2\bar{\alpha}^2}{(1+\bar{p})}\cos 2\theta \\ n_x &= \bar{\alpha}\left\{\left[1 - \frac{\chi^2\bar{\alpha}^2}{4(1+\bar{p})}\right]\cos\theta - \frac{\chi^2\bar{\alpha}^2}{12(1+\bar{p})}\cos 3\theta\right\} \end{aligned} \tag{40}$$

Then the stipulation that the maximum compressive stress ($\theta = 0$) must remain below the critical buckling stress to remain stable

$$\frac{N_x(\theta=0)}{H} < \frac{-2\sqrt{D_{11}E_\theta H}}{H}\left[\frac{1}{R} + \kappa_\theta(\theta=0)\right] \tag{41}$$

generates the stability criterion for orthotropic tubes of arbitrary length

$$\bar{\alpha}\left[1 - \frac{\chi^2\bar{\alpha}^2}{3(1+\bar{p})}\right] < 1 - \frac{\chi^2\bar{\alpha}^2}{(1+\bar{p})} \tag{42}$$

Thus, the method for finding the critical bending curvature of an orthotropic cylinder with internal pressure consists of finding the root of a third-degree polynomial. One interesting point here is that for certain values of χ (and $\bar{p}$), the critical curvature for buckling is not reached until after the maximum moment is attained. Some comparisons of Eqs. (37) and (42) will be made in the next sections to illustrate this point.

Lastly, these collapse points will be compared in terms of curvatures as opposed to applied bending moments. This enables us to distinguish between collapse criteria more accurately, since moments near the limit point tend to have similar values because of the small slope of the load–displacement curve (see Fig. 3).

Influence of Laminate Stacking Sequence

Brazier's analysis applied to long cylinders constructed of orthotropic material was first done by Kedward.[15] For our analysis, the nondimensional parameter χ of Eq. (33) seems to describe a measure of orthotropy for any shell wall construction. However, χ does not signify any classical measure of orthotropy, such as the ratio of the moduli in perpendicular directions. For instance, isotropic materials and cylinders fabricated from one layer of an orthotropic material both possess a value of $\chi = 1$. Clearly then, the degree of orthotropy of the material is not represented by χ. A more accurate description of χ is related to the collapse loads of the cylinder. Recall that the classical buckling moment is proportional to $\sqrt{(D_{11}E_\theta)}$. However, because of the Brazier effect, another mode of failure exists in the form of a limit moment on the nonlinear load path. After unnormalizing Eq. (37), it can be shown that this limit load is proportional to $\sqrt{(D_{22}E_x)}$. This makes physical sense, since each of the stiffness measures E_x and D_{22} contribute to the nonlinearity in different ways: a high axial in-plane stiffness resists the curving of the tube that generates the inward forces that ovalize the cross section; whereas a large circumferential bending stiffness will not allow the circular cross section to deform into an oval. Therefore, χ is an indication of the ratio between the buckling and limit loads of a tube under bending and will be dubbed the collapse parameter. Structures with a low collapse parameter will become locally unstable before the limit point is reached, whereas tubes with large values of χ will attain a maximum moment before buckling occurs.

The question still remains as to what kind of structures generate different values of the collapse parameter defined by Eq. (33). The ratio of bending stiffness divided by the in-plane stiffness in two perpendicular directions is certainly not intuitive. As mentioned previously, any tube constructed of a single orthotropic layer will behave the same with respect to its normalized collapse load values. The objective is to find structures that possess drastically different bending and in-plane stiffness characteristics in the axial and circumferential directions. Obviously, both multilayered composites and directionally stiffened cylinders satisfy this criterion and can achieve a wide range of χ values. For instance, a simple laminate composed of unidirectional orthotropic layers ($E_1/E_2 \approx 11$) with the layup $[0_2/\pm 45]_s$ has a collapse parameter χ equal to 1.55. Including the

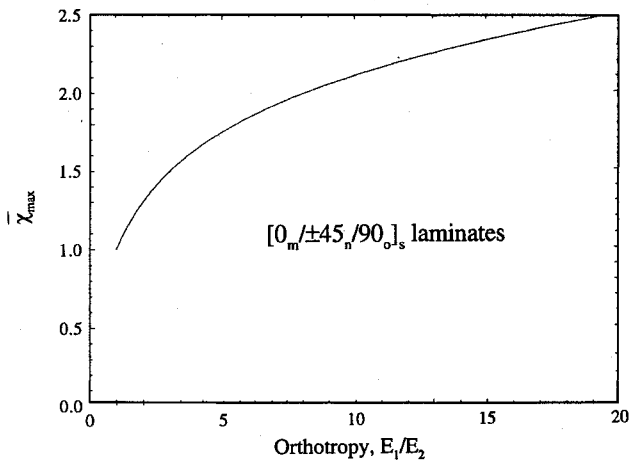

Fig. 4 Maximum collapse parameter vs material orthotropy.

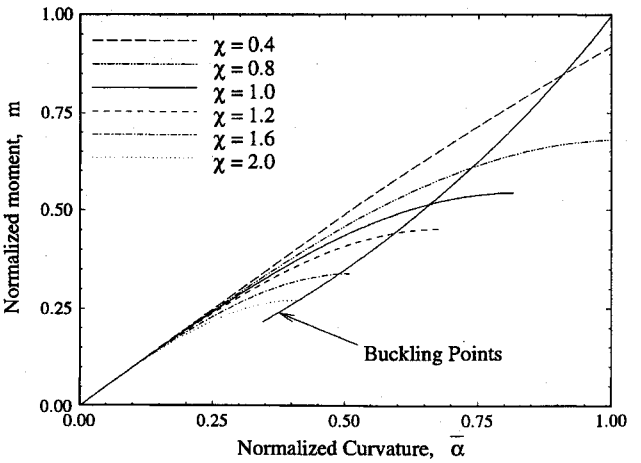

Fig. 5 Moment vs curvature for long orthotropic cylinders.

effects of smeared ring stiffeners or longitudinal stringers can lead to an even greater range of collapse parameters. Therefore, the collapse parameter is a direct function of the stacking sequence of multilayered and/or stiffened shells, as well as the material properties of the constituent layers.

Some preliminary optimization has been performed to determine the maximum value of χ that can be achieved as a function of lamina orthotropy and stacking sequence. Laminates were restricted to be symmetric, balanced, and constructed only of 0-, ±45-, and 90-deg plies. It was found that laminates with large values of χ tend to have many 0-deg plies at the extreme locations of the laminate, with 90 deg plies at the midplane and a transition region of ±45-deg plies between the two. Conversely, small values of χ are generated by an inner core of 0-deg plies with 90-deg layers at the extremities.

The extreme value of the collapse parameter for these optimal ply configurations also depends on the orthotropy of the laminae. A plot of the maximum value of χ as a function of material orthotropy is shown in Fig. 4 (here we assumed that the shear modulus of the lamina was that of the matrix material). The amount of 0- and 90-deg plies also changed as a function of material orthotropy, whereas the percentage of ±45-deg layers remained about the same (around 10%). Two mechanisms to increase the value of χ were observed. For smaller values of E_1/E_2, the laminate was composed of over 50% 90-deg layers in the core of the laminate. This has the effect of making E_θ greater than E_x without a large difference in the bending stiffnesses. However, the maximum values of χ are not very large for this case because of the small value of the orthotropy. As the orthotropy increases, the mechanism to maximize χ changes. The amount of 0-deg plies at the extreme locations of the laminates grows to almost 60%, thereby increasing the bending stiffness in the axial direction (D_{11}) when compared with that in the circumferential direction (D_{22}) because of the distance of these plies from the laminate midplane. Analogous optimization techniques for minimum values of χ would result in a reversal of these trends, and the curve in Fig. 4 would follow an inverse relation (i.e., $\chi_{min} = 1/\chi_{max}$).

Representative moment vs curvature relations calculated from the linearized solution of Eq. (36) for various values of the collapse parameter χ are displayed in Fig. 5 for unpressurized cylinders. The load paths are terminated when the limit point is encountered. The intersection of the solid line with a load path represents the buckling point according to the Seide–Weingarten criterion.[14] Note in Fig. 5 that the tubes with higher values of the collapse parameter experience significant nonlinearity because of the Brazier effect before a buckling point is attained. Conversely, laminates possessing a small value of χ behave more linearly and collapse when their classical buckling value is reached. Thus the limit point of the Brazier effect cannot be used as an accurate estimate of the collapse load for long cylinders possessing a small value of χ. To illustrate this more clearly, critical curvatures according to limit load and local instability are plotted as a function of χ in Fig. 6. The lower value of the two is the curvature that determines collapse. Note that for small

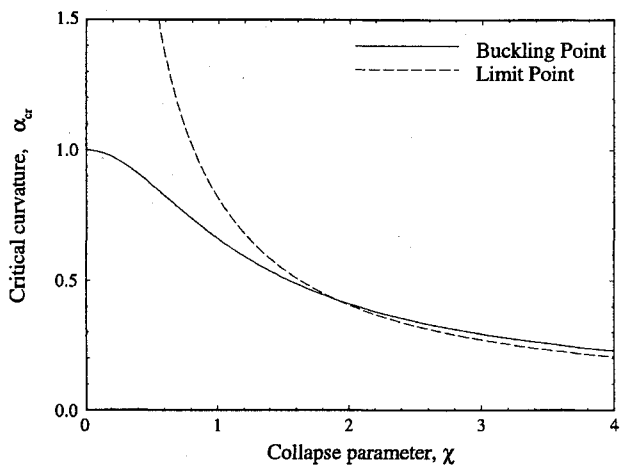

Fig. 6 Buckling curvature and limit curvature vs collapse parameter.

values of χ, the limit moment is not an accurate estimate of the collapse load. Furthermore, for values of χ greater than 2, the limit point is actually locally stable! However, it may be almost impossible to distinguish the limit load behavior from the local instability experimentally, for the buckling load remains very close to the limit load, and the catalyst to the postbuckled state may be difficult to distinguish.

Influence of Pressure

Internal or external pressure can also affect the amount of nonlinearity for long tubes under bending. Plots of load–displacement curves are displayed in Fig. 7 for typical values of pressure for shells with a collapse parameter equal to 1. A large internal pressure creates circumferential stresses that will dominate the bending stresses in the tube and forces the cross section to remain circular. Thus the ovalization that lowers the moment of inertia will not occur, and the nonlinearity as a result of the Brazier effect will be lessened. Conversely, exterior pressure heightens the nonlinear effect by encouraging the cross-sectional deformation to increase. The solid line in Fig. 7 again corresponds to the buckling point using the Seide–Weingarten criterion.[14]

Limit points and buckling loads are also compared as a function of pressure in Fig. 8. Note that the pressure has been normalized with respect to a classical buckling value for a circular ring under external pressure (see Ref. 16). A value of $\bar{p} = -1$ would result in bifurcation of the tube before a bending moment is ever applied. However, large external pressures also increase the Brazier effect, so that a limit point may occur first.

This effect of pressure on collapse loads for cylinders under bending was first investigated in detail by Fabian,[10] who also performed

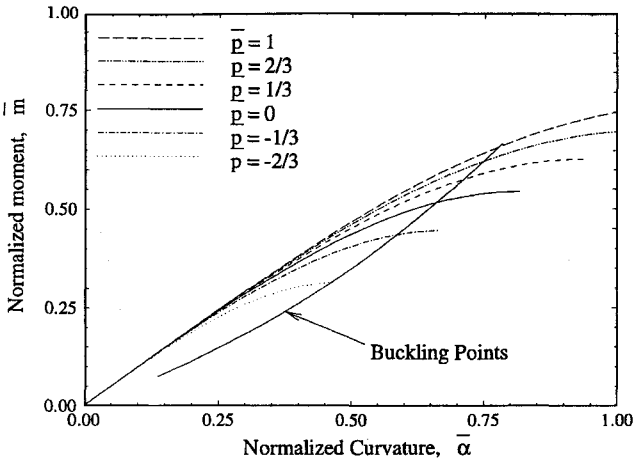

Fig. 7 Moment vs curvature for pressurized isotropic cylinders.

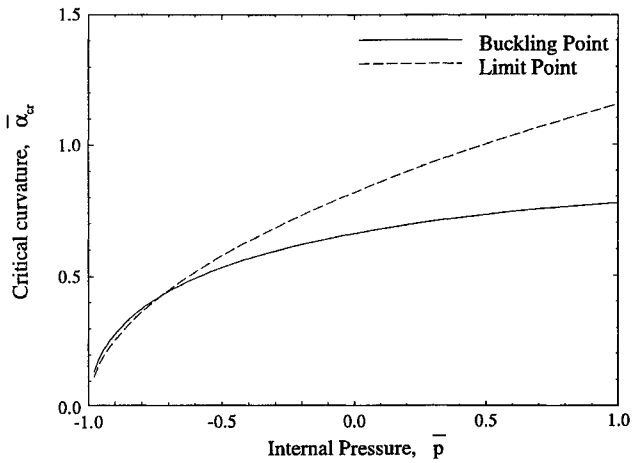

Fig. 8 Buckling curvature and limit curvature vs pressure.

a full bifurcation analysis from the deformed state for infinite cylinders under bending, pressure, and axial loads. He discovered that the failure mode depends on the radius-to-thickness ratio of the cylinder and that thicker cylinders tend to collapse because of the limit load failure, whereas thin shells approach the engineering approximation of Seide and Weingarten.[14] Our simplified bifurcation analysis, based on the buckling stress calculation of Seide and Weingarten, does not depend on the radius-to-thickness ratio of the tube; therefore Fabian's results[10] cannot be verified using our assumptions. However, we can conclude from our simplified analysis that the limit load is again a poor estimate of the failure load of the structure except for extreme cases.

Conclusions

The governing equations for the bending response of orthotropic infinite length cylinders have been presented. The analysis presented here yields a complete nonlinear formulation of the Brazier effect from semimembrane nonlinear shell theory. The nonlinear effect has been introduced in a rigorous manner consistent with classical shell theory. Numerical and analytical solutions of the differential equation were found to agree excellently, and the load–displacement response, as well as the collapse behavior of these structures, was found to depend strongly on laminate stacking sequence and internal pressure. A nondimensional collapse parameter that distinguishes between shells with a propensity to buckle from those that experience limit load behavior was also introduced. Finally, it was demonstrated that, in general, the limit point in the load–deflection curve could not be used as a reliable estimate of the collapse load of the structure.

Acknowledgment

The work reported was supported in part by Grant NAG-1-643 from NASA Langley Research Center. The support for the work of the first two authors is gratefully acknowledged.

References

[1]Brazier, L. G., "The Flexure of Thin Cylindrical Shells and Other 'Thin' Sections," *Late of the Royal Aircraft Establishment*, Repts. and Memoranda 1081 (M.49), Vol. 213, Royal Society of Aeronautics, 1926, p. 187.

[2]Brazier L. G., "On the Flexure of Thin Cylindrical Shells and Other Thin Sections," *Proceedings of the Royal Society of London, Series A: Mathematical and Physical Sciences*, Vol. 116, 1927, pp. 104–114.

[3]Vasiliev, V. V., *Mechanics of Composite Structures*, Taylor and Francis, Washington, DC, 1993, pp. 406–409.

[4]Aksel'rad, E. L., and Emmerling, F. A., "Collapse Load of Elastic Tubes Under Bending," *Israel Journal of Technology*, Vol. 22, 1984/85, pp. 89–94.

[5]Libai, A., and Bert, C. W., "A Mixed Variational Principle and Its Application to the Nonlinear Bending Problem of Orthotropic Tubes—Part I. Development of General Theory and Reduction to Cylindrical Shells, Part II. Application to Nonlinear Bending of Circular Cylindrical Tubes," *International Journal of Solids and Structures*, Vol. 31, No. 7, 1994, pp. 1019–1033.

[6]Corona, E., and Rodrigues, A., "Bending of Long Cross-Ply Composite Circular Cylinders," *Composites Engineering*, Vol. 5, No. 2, 1995, pp. 163–182.

[7]Jones, R. M., *Mechanics of Composite Materials*, Hemisphere, Washington, DC, 1975, pp. 147–152.

[8]Novoshilov, V. V., *The Theory of Thin Shells*, translated by P. G. Lowe, Noordhoff International, Leyden, The Netherlands, 1959, pp. 6–14.

[9]Reissner, E., "On Finite Bending of Pressurized Tubes," *Journal of Applied Mechanics*, Vol. 26, Sept. 1959, pp. 386–392.

[10]Fabian, O., "Collapse of Cylindrical, Elastic Tubes Under Combined Bending, Pressure, and Axial Loads," *International Journal of Solids and Structures*, Vol. 13, 1977, pp. 1257–1270.

[11]Wood, J. D., "The Flexure of a Uniformly Pressurized Circular, Cylindrical Shell," *Journal of Applied Mechanics*, Vol. 80, Dec. 1958, pp. 453–458.

[12]Calladine, C. R., *Theory of Shell Structures*, Cambridge Univ. Press, Cambridge, England, UK, 1983, pp. 605–625.

[13]Aksel'rad, E. L., "Pinpointing the Upper Critical Bending Load of a Pipe by Calculating Geometric Nonlinearity," *Akademiya Nauk SSSR, Izvestiya Mekhanika*, Vol. 4, 1965, pp. 133–139.

[14]Seide, P., and Weingarten, V. I., "On the Buckling of Circular Cylindrical Shells Under Pure Bending," *Journal of Applied Mechanics*, Vol. 28, March 1961, pp. 112–116.

[15]Kedward, K. T., "Nonlinear Collapse of Thin-Walled Composite Cylinders Under Flexural Loading," *Proceedings of the 2nd International Conference on Composite Materials* (Toronto), Metallurgical Society of AIME, Warrendale, PA, 1978, pp. 353–365.

[16]Brush, D. O., and Almroth, B. O., *Buckling of Bars, Plates, and Shells*, McGraw–Hill, New York, 1975, pp. 135–137.